MOLECULAR AND CELLULAR BIOLOGY, Dec. 1996, p. 7133–7143 Vol. 16, No. 12
0270-7306/96/$04.00+0

A Mutation in Mouse *rad51* Results in an Early Embryonic Lethal That Is Suppressed by a Mutation in *p53*

DAE-SIK LIM† AND PAUL HASTY†*

Department of Biochemistry and Molecular Biology, M. D. Anderson Cancer Center, Houston, Texas 77030

Received 15 July 1996/Returned for modification 3 September 1996/Accepted 10 September 1996

RecA in *Escherichia coli* and its homolog, ScRad51 in *Saccharomyces cerevisiae*, are known to be essential for recombinational repair. The homolog of RecA and ScRad51 in mice, MmRad51, was mutated to determine its function. Mutant embryos arrested early during development. A decrease in cell proliferation, followed by programmed cell death and chromosome loss, was observed. Radiation sensitivity was demonstrated in trophectoderm-derived cells. Interestingly, embryonic development progressed further in a *p53* null background; however, fibroblasts derived from double-mutant embryos failed to proliferate in tissue culture.

The repair of double-strand breaks (DSB) in DNA is an essential cellular process that spans the evolutionary scale and that may occur during general cellular functions such as DNA repair or during species-specific cellular functions such as mating-type switch in *Saccharomyces cerevisiae* and V(D)J (variable [diversity] joining) recombination in mammals (for reviews, see references 23, 29, and 69). In bacteria and yeast cells, DSB are predominantly repaired by a homologous recombination pathway (42, 54).

In the budding yeast *S. cerevisiae*, repair of DSB occurs through a homologous recombination pathway that depends on the RAD52 epistasis group (Rad50 to Rad57), which was identified in cells sensitive to ionizing radiation. Some members of this group were shown to be important for recombinational repair during mitotic and meiotic recombination (for reviews, see references 23, 24, and 61). Among the members of the RAD52 epistasis group, ScRad51 is interesting because of its similarity to an *Escherichia coli* recombination protein, RecA (1, 6, 75). They have approximately 30% homology in about 220 amino acids and polymerize on double-stranded and single-stranded DNA, showing a nearly identical helical filament (60). ScRad51 and RecA catalyze an ATP-dependent strand exchange between homologous DNA molecules (63, 78, 79).

ScRad51 repairs DSB by recombination. DSB accumulate at recombination hot spots in cells that lack ScRad51 during meiosis (75). ScRad51 and another RecA homolog, DMC1, colocalize to meiotic nuclei (10) and promote meiotic chromosome synapsis (68). Therefore, ScRad51 may mediate meiotic recombination by binding to single strands generated at DSB, which could lead to pairing and strand exchange during meiosis, as suggested by Sung and Robberson (79).

RecA and ScRad51 homologs have been discovered in a wide range of organisms, including the fission yeast *Schizosaccharomyces pombe* (36, 56, 74), lilies (82), chickens (9), mice (53, 74) and humans (74, 89), and appear to be involved in DNA repair and recombination on the basis of the following indirect evidence. (i) Conserved RecA homology: MmRad51 is 83% homologous and 69% identical to ScRad51 and 51% homologous and 28% identical to RecA. The level of homology between mammalian and yeast Rad51 suggests conserved function because of the remarkable similarity between other mammalian and yeast repair pathways (for a review, see reference 16). (ii) Expression pattern: *MmRAD51* is highly expressed in tissues involved in meiotic recombination (i.e., testes and ovaries) (53, 74), and expression of the *S. pombe* homolog, *SpRAD51* (also called *rhp51*$^+$), increased after cells were treated with methyl methanesulfonate, suggesting a role in DNA repair (36). (iii) Protein cellular localization: Mouse, chicken, and lily Rad51 localized as discrete foci on meiotic chromosomes at varying concentrations during prophase 1, possibly on the lateral elements and recombination nodules, suggesting a role in the repair of DSB during meiotic recombination (3, 28, 82). Human Rad51, HsRad51, migrated to the nucleus with increasing concentration after exposure to DNA-damaging agents, suggesting a repair function (82). (iv) Filament formation on DNA: HsRad51 bound to single-stranded DNA demonstrating a potential for strand exchange (8).

To date there is no direct evidence to describe MmRad51 function. MmRad51 was mutated by the embryonic stem (ES) cell and gene-targeting technology to directly test its function in mice. The mutant embryos arrested in development shortly after implantation. There was a decrease in cell proliferation followed by programmed cell death, and trophectoderm-derived cells were sensitive to gamma radiation. Severe chromosome loss was observed in most mitotically dividing cells. The mutant embryos lived longer and developed further in a *p53* mutant background; however, double-mutant embryonic fibroblasts failed to proliferate in tissue culture, reflecting the embryos' limited life span.

MATERIALS AND METHODS

Generation of the *rad51*^{MI} mutation. All the vectors were constructed from the same genomic clone isolated from a 129/SvEv library (Stratagene). The exon-intron boundaries were determined and labeled *a* to *e* because the first exon was not found in this genomic fragment. Exon *b* is the first coding exon. DVhygro and DVpuro contain 7 kb of homologous sequences from *Kpn*I to *Xho*I (engineered), and a 300-bp *Sac*I-*Eco*RI fragment was replaced with a positive selection cassette. Exon *d* was deleted. DVpuro2 contains 6.8 kb of homologous sequences from *Eco*RI to *Xho*I, and a 1.7-kb *Sac*I-*Eco*RI fragment was replaced with a positive-selection cassette. An internal *Kpn*I site was destroyed. The positive-selection cassette was PGKpurobpA for DVpuro and DVpuro2 which contained the puromycin *N*-acetyltransferase gene (51). The positive-selection cassette was PGKhygrobpA for DVhygro which contained the hygromycin B phosphotransferase gene (11). Both PGKpurobpA and PGKhygrobpA contained the phosphoglycerate kinase 1 promoter *pgk-1* (2) and the bovine growth hormone polyadenylation sequence *bpA* (62). The negative-selection cassette was MCltk (50).

AB1 ES cells were transfected with the targeting vectors and cultured as previously described on a monolayer of mitotically inactivated SNL 76/7 STO cells (12). Cells were grown in M15 (15% fetal calf serum from HyClone,

* Corresponding author.
† Present address: Lexicon Genetics Incorporated, 4000 Research Forest Dr., The Woodlands, TX 77381.

Dulbecco's modified Eagle's medium from Gibco, 10^{-4} M β-mercaptoethanol, 2 mM L-glutamine, 49.5 U of penicillin per ml, and 38.8 μg of streptomycin per ml). Cells were trypsinized and resuspended in phosphate-buffered saline (PBS) (Ca^{2+} and Mg^{2+} free). Transfection was performed by electroporation of 10 μg of vector cut with *Kpn*I (in the polylinker) in PBS containing 10^7 cells per ml at 230 V and 500 μF with a Bio-Rad gene pulser. One electroporation was plated onto four 10-cm-diameter plates, and positive and negative selection media were added 24 h later. For DVpuro and DVpuro2, a final concentration of 3 μg of puromycin per ml was used for positive selection, and for DVhygro a final concentration of 200 μg of hygromycin per ml was used for positive selection. For all vectors, a final concentration of 0.2 μM FIAU [1-(2′-deoxy-2′-fluoro-β-D-arabinofuranosyl)-5-iodouracil] was used for negative selection. After 9 days in selection, colonies were picked for Southern analysis.

Southern and PCR analysis. Genomic DNA was extracted from ES cells for Southern analysis by the microextraction procedure (64). *Eco*RV-digested DNA, separated by electrophoresis through a 0.7% gel in TAE buffer (0.04 M Tris-acetate, 0.001 M EDTA), was transferred to a Hybond-N+ filter (Amersham) and hybridized to random primed labeled probe (exon *a*) according to the manufacturer's specific conditions (Amersham).

Three primers were used in the PCR mixture. The 5′ sense primer to the *MmRAD51* intron upstream of exon *d* (5′-AATCACAGTCTAAAGCATTTTG G-3′) was used to detect both wild-type and mutant alleles. The 3′ antisense primers to exon *d* (5′-GCTTGTCCAGCTCTTTGGAGCCA-3′) and the *pgk-1* promoter (5′-CCAAGGCCTACCCGCTTCCATT-3′) were used to detect the wild-type and mutant alleles, respectively. The PCR was performed with 35 cycles of amplification at 94°C for 30 s, 57°C for 1 min, and 72°C for 1 min in a Perkin-Elmer DNA thermal cycler 480. Fragments of 270 bp (wild type) and 450 bp (mutant) were generated. The fragments were separated in a 1% agarose gel in TAE buffer by electrophoresis. To prove the fragments were not artifacts, they were transferred to a Hybond-N+ filter (Amersham) and hybridized to an internal sense oligonucleotide (5′-TGGTGAAACCCATTGGAACCAA-3′) end labeled with γ-ATP (not shown).

The genotypes of cells from mouse tails, yolk sacs, embryos, and histological sections and the genotypes of cultured trophoblast-like cells were determined by PCR amplification of genomic DNA. DNA samples were prepared from embryos as described by Imamoto and Soriano (35). DNA was prepared from histological sections after completion of BrdU (5-bromo-2′-deoxyuridine) labeling and a terminal deoxynucleotidyltransferase-mediated dUTP-biotin nick end labeling (TUNEL) assay. The embryonic cells were isolated from the maternal cells by scraping the maternal component off the slide with a 25G5/8 needle. A hydrophobic slide marker (PAP PEN from Kiyota Express) was used to draw a barrier around the embryo. Lysis buffer was added directly to the embryo and removed 10 min later. The contents in the lysis buffer were then processed as described by Imamoto and Soriano. Half of the product was used for PCR, and hybridization was needed to easily visualize the amplified fragments. The genotypes of embryonic cells to be used in the gamma radiation experiment were determined by PCR. On day 7, the trophoblast-like cells and floating embryos were lysed. The genotypes of embryos used for the acridine orange stain and for metaphase spreads were initially determined by size and then confirmed by PCR on a subset of cells.

Genotype determination of *p53* was performed as described previously (19) with genomic DNA isolated from either tails, whole embryos, yolk sacs, or murine embryonic fibroblasts (MEF). *Bam*HI-digested DNA was separated by agarose gel electrophoresis and hybridized to exons 2 to 6 from cDNA. Only about 1 to 2 μg of DNA was generated from the yolk sacs of 8.5-day-old embryos; therefore, about 5 ng was used for the genotype determination of MmRAD51 by PCR and the remainder was digested with *Bam*HI and loaded in a small well (1.5 mm by 3 mm) for the genotype determination of *p53* by Southern analysis.

Analysis of an MmRAD51 transcript. mRNA was isolated from embryonic day (E) 7.0 embryos by using the lysate mRNA capture kit for reverse transcriptase PCR (Amersham). Briefly, after embryos were incubated in lysis solution for 5 min with 4 M guanidium thiocynate, the membrane was incubated with cell lysate to capture mRNA for 30 min at room temperature. The membrane was rinsed three times with 1× PCR buffer, and reverse transcription was performed with random hexamer primers and reverse transcriptase for 30 min at 42°C. The total volume was increased by adding H_2O to 100 μl. The quantity of mRNA was roughly estimated by measuring the PCR amplification product with glyceraldehyde-3-phosphate dehydrogenase (GAPDH) primers on 2 μl of the final solution after 30 cycles. The amplified products were observed on a 1% agarose gel after electrophoresis. PCR was done for GAPDH with the following primers: 5′ sense primer, 5′-AAGGTCATCCCAGAGCTG-3′; 3′ antisense primer, 5′-GCCATG AGGTCCACCACCCT-3′. PCR was done for *XRCC5* with the following primers: 5′ sense primer, 5′-ATGGGTAACTCCATTCCTGGTGAA-3′; 3′ antisense primer 5′-TTGAGGAAAGGAGGGTTTGAG-3′. PCR was performed for *MmRAD51* with the following primers: 5′ sense primer, 5′-ATGGCTATGCAA ATGCAGCTT-3′; 3′ antisense primer, 5′-AAACATCTCTGTGATAGATCC-3′. The *MmRAD51* PCR product was transferred to a Hybond-N+ filter (Amersham) and hybridized to an internal oligonucleotide probe, 5′-CCACTGTATG GTACCCAA-3′. PCR conditions were 93°C for 30 s, 59°C for 1.5 min, and 72°C for 1 min for 30 cycles.

Histological analysis and BrdU labeling. Embryos were fixed in 10% buffered formalin, processed, and embedded in paraffin by using standard procedures (38). Sagittal sections (7 μm thick) were cut and stained with hematoxylin and eosin. At E5.5, 5 rad^{M1} mutant and 13 control embryos were observed. At E6.5 three rad^{M1} mutant and eight control embryos were observed. At E7.5 four rad^{M1} mutant and nine control embryos were observed.

BrdU labeling was performed as described by Hayashi and colleagues (33). Pregnant females were injected intraperitoneally with BrdU (100 μg of BrdU per g of body weight) and sacrificed 25 min later for E5.5 embryos or 70 min later for E6.5 and E7.5 embryos. Embryos were processed for histology. The sections were incubated with 0.02% pepsin (Sigma) in 0.01 N HCl for 20 min at 37°C. DNA was denatured with 2 N HCl for 45 min at room temperature and neutralized with 0.1 M sodium borate. The sections were incubated with anti-BrdU antibody (Amersham cell proliferation kit) for 60 min at room temperature, washed with PBS, and incubated with peroxidase anti-mouse immunoglobulin G for 30 min. After washes in PBS, sections were visualized with DAB (3,3′-diaminobenzidine) and counterstained with hematoxylin. Quantitation was performed by counting BrdU-labeled and unlabeled (hematoxylin-stained) cells. At E5.5, 5 rad^{M1} mutant and 13 control embryos were observed. At E6.5 three rad^{M1} mutant and five control embryos were observed. At E7.5 four rad^{M1} mutant and four control embryos were observed.

Cell death analysis. A TUNEL assay was performed on histological sections of E6.5 and E7.5 embryos (25). The TUNEL reaction kit (Boehringer Mannheim) was used according to instructions to detect incorporation of fluorescein-dUTP mediated by terminal transferase. Briefly, sections were incubated with proteinase K (20 μg/ml in 10 mM Tris-HCl, pH 7.5) for 20 min at 37°C and washed with PBS. The sections were then incubated with 50 μl of TUNEL reaction mixture for 60 min at 37°C. After being washed with PBS, samples were directly analyzed under a Leitz Laborlux S fluorescence microscope. At E6.5 two rad^{M1} mutant and two control embryos were observed. At E7.5 three rad^{M1} mutant and three control embryos were observed.

Embryo culture and radiation analysis. Blastocysts were isolated 3.5 days after a $rad51^{M1+/-}$ cross by standard procedures (day zero). On day zero, embryos were exposed to gamma radiation in a ^{137}Cs gamma irradiator and then plated onto a 6-cm-diameter gelatinized plate and allowed to attach in M15 medium. The trophoblast-like cells were counted on day 7.

Measurement of DNA content. Metaphase spreads were performed after an intraperitoneal injection of colcemid (2 μg per g of body weight; Sigma) to pregnant females 2 h before they were sacrificed. Chromosome staining was performed by an air-drying method on cells derived from E7.5 embryos as described previously (81). Disaggregated cells from embryos were incubated with 1% hypotonic sodium citrate for 30 min at 37°C. After fixation for 5 min in 3:1 ethanol-acetic acid solution, cells were spread on a grease-free slide, dried for 2 h, and prestained with 2% orcein in 50% lactic acid. Slides were rinsed with a 50% lactic acid-acetic acid solution and subsequently stained with 2% orcein and examined under a microscope.

An acridine orange stain (27) was performed on cells derived from E7.5 embryos. Three $rad51^{M1-/-}$ embryos were trypsinized together, and three control embryos were trypsinized individually. Half of the sample was used for genotype determination by PCR, and half was stained with acridine orange (0.3 μg/10 μl). The cells were immediately viewed with a Leitz Laborlux S fluorescence microscope (magnification, ×50). The film was exposed under oil immersion at 400 ASA with the spot setting to isolate a single cell. Genetic content was grossly measured by fluorescence emission as determined by exposure time: the longer the time, the less DNA. MEF derived from three control E9.5 embryos and one $p53^{-/-}$ $rad51^{M1-/-}$ embryo were also observed by a similar technique.

MEF generation and culture. To generate MEF, E8.5 and E9.5 embryos were isolated and incubated in 50 μl of trypsin for 15 min and then disaggregated by pipetting after the addition of 50 μl of M10 (10% fetal calf serum from HyClone, Dulbecco's modified Eagle's medium from Gibco, 2 mM L-glutamine, 49.5 U of penicillin per ml, 38.8 μg of streptomycin per ml). The cells were plated onto 15-mm-diameter plates and grown in M10. The cell number was counted after 6 days in tissue culture. The control cells were counted with a hemacytometer, and the double-mutant cells were counted directly under a light microscope because there were too few cells to use a hemacytometer. The control and double-mutant MEF were then passaged at low density. Control cells were plated at varying concentrations (100, 500, 1,000, 2,000, and 4,000 cells on a 35-mm-diameter plate or 3,000 cells on a 90-mm-diameter plate). Each isolate of double-mutant cells was plated onto a single 35-mm-diameter plate. The control and double-mutant cells were counted the next day under a light microscope to determine the cell densities. After 14 days in tissue culture, the plates were stained with crystal violet to identify colonies of 4 to 16, 17 to 50, and >50, cells. For controls, colonies were counted on only those plates with cells at the same approximate densities as those on plates with double-mutant cells.

RESULTS

Generation of a mutation in *MmRAD51*. An out-of-frame deletion was introduced into *MmRAD51* in ES cells by gene targeting. A deletion vector, DVpuro, was used to delete nucleotides 413 to 530, which code for amino acids 73 to 112 (74) and frameshift the downstream sequences (Fig. 1A). DVpuro

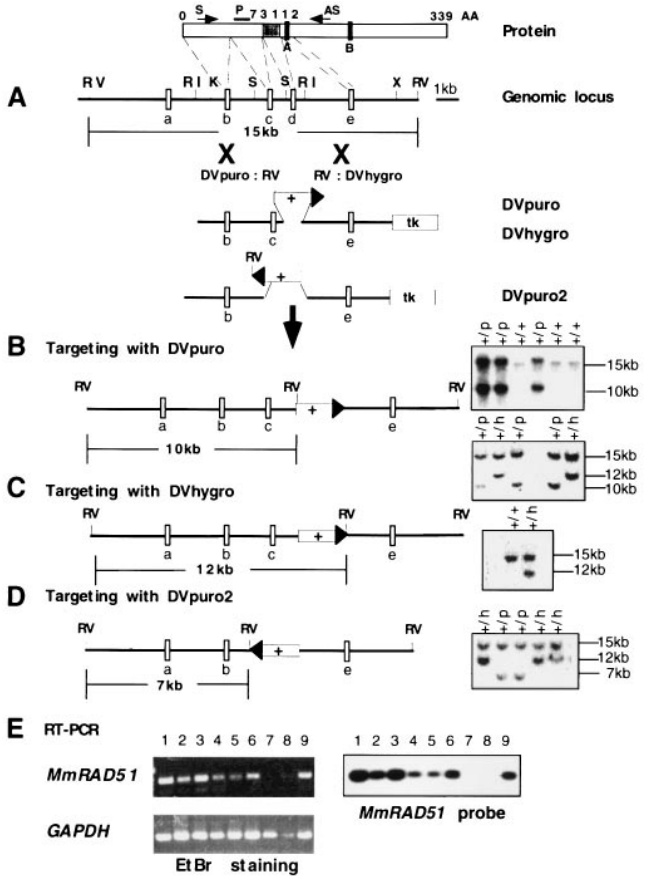

FIG. 1. Genomic structure and targeting of *MmRAD51*. (A) Exons were labeled a to e because the 5′ mRNA sequences were not located in this genomic fragment and the first exon was not known. A and B represent the Walker A- and B-type nucleotide-binding domains. Positive-selection cassettes are indicated by boxes labeled +. Negative-selection cassettes, designated MCltk, are indicated by boxes labeled tk. All vectors were linearized with *Kpn*I (K) in the polylinker. Exon a was the probe. *Eco*RI, RI; *Eco*RV, RV; *Sac*I, S. Sense and antisense primers for RT-PCR are indicated by arrows labeled S and AS, respectively. The oligonucleotide probe for RT-PCR (P). (B) Targeting with DVpuro (p). Upper panel, genomic DNA extracted from tails of mice. The wild-type (+/+) 15-kb *Eco*RV fragment was reduced to 10 kb (+/p). Lower panel, genomic DNA extracted from ES cells previously targeted with DVhygro (+/h). (C) Targeting with DVhygro (h). A 12-kb *Eco*RV fragment was produced (+/h). (D) Targeting with DVpuro2 into a cell line previously targeted with DVhygro. A 7-kb *Eco*RV fragment was produced. (E) RT-PCR analysis of E7.0 embryos. Left panels, ethidium bromide (EtBr)-stained agarose gels. Right panel, autoradiograph after hybridization to oligonucleotide probe. Lanes 1 to 6 and 9, controls; lanes 7 and 8, mutants.

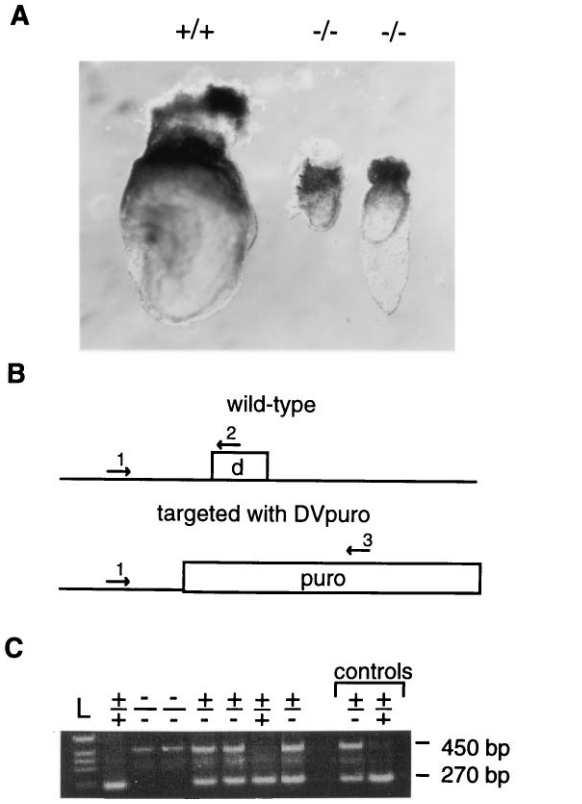

FIG. 2. E7.5 control and *rad51*$^{M1-/-}$ embryos. (A) Wild type, +/+; mutant, −/−. Magnification, ×16. (B) Genotype determination for embryos by PCR. The sense primer for the wild-type and targeted copies is designated 1. The antisense primer for the wild-type copy in exon d is designated 2. The antisense primer for the targeted copy in the *pgk-1* promoter is designated 3. Mutant band, 450 bp; wild-type band, 270 bp. (C) Ethidium bromide-stained gel of the PCR mixture. Wild-type, +/+; mutant, −/−; heterozygote, +/−. DNA controls were extracted from *rad51*$^{M1+/-}$ and wild-type ES cells. The fragments were hybridized to an internal probe (not shown). A minor band was observed between the 450- and 270-bp bands; however, this band did not hybridize to the internal probe and disappeared at a higher annealing temperature.

was transfected into ES cells by electroporation, and clones resistant to positive and negative selection media (50) were screened by Southern analysis to identify targeted clones (Fig. 1B). Mice with this *rad51* mutation (designated *rad51*^{M1}) were generated with two targeted clones. Both clones (129/SvEv origin) were transmitted through the germ line after chimeras were crossed with C57BL/6 females. Mice generated from either clone displayed the same phenotype; therefore, these data were combined. There were no obvious defects observed in *rad51*$^{M1+/-}$ mice. However, *rad51*$^{M1-/-}$ mice were not produced out of 75 newborns generated from F1 heterozygous crosses.

The consequences of the *rad51*^{M1} mutation on *MmRAD51* transcript levels was determined by RT-PCR on mRNA isolated from control and mutant E7.0 embryos (Fig. 1E). *GAPDH* and *XRCC5* transcript levels were measured to control for mRNA loading, and both transcripts were detected in control and mutant embryos. *MmRAD51* mRNA was detected in control but not mutant embryos, even after hybridization with an internal oligonucleotide probe. The out-of-frame deletion and the lack of *MmRAD51* mRNA make it likely that the *rad51*^{M1} mutation was null and that this mutation was lethal in the homozygous condition.

***rad51*$^{M1-/-}$ embryos arrest early in development.** When do mutant embryos die? Timed heterozygous matings were performed, and females were sacrificed 3.5 to 8.5 days later. Control and *rad51*$^{M1-/-}$ embryos were the same gross size at E3.5 to E6.0. However, at E7.5, control embryos were much larger than mutant embryos which appeared to arrest 24 to 36 h earlier (Fig. 2A; Table 1). Some mutant embryos began to resorb by E7.5. The genotypes of the embryos were determined by PCR (Fig. 2B, C).

Histological analysis was performed on E5.5, E6.5, and E7.5 embryos (Fig. 3). After the histological analysis was complete, the genotypes of the sections were determined by PCR. *rad51*$^{M1-/-}$ embryos were hypocellular with abnormal cellular morphology; the cells were cuboidal in shape on transverse section. Mutant embryos arrested at the early egg cylinder stage, typically observed by E5.5 in control embryos. The proamniotic cavity was present in most control and mutant em-

TABLE 1. Genotypes[a] and gross morphology for E3.5 to E8.5 embryos

E	No. of embryos with indicated genotype (gross morphology[b])		
	+/+	+/−	−/−
3.5	25 (N)	51 (N)	27 (N)
6.5	5 (N)	11 (N)	5 (N)
7.5	11 (N)	17 (N)	6 (S), 5 (R)
8.5	5 (N)	12 (N)	6 (R)

[a] The genotypes of all embryos were determined by PCR, except for four of the six resorbed embryos at E8.5. There was not enough embryonic material for determinations of the genotypes of these four embryos, and so they were presumed to be mutant.

[b] Gross morphology designations: N, normal; S, small; R, resorbed.

bryos by E5.5; however, the amniotic cavity and mesoderm failed to develop in mutant embryos. The hypocellular condition and arrested development indicated reduced cell proliferation.

To observe cell proliferation, E5.5, E6.5, and E7.5 embryos were labeled with BrdU. A lower percentage of cells incorporated BrdU in *rad51*$^{M1-/-}$ embryos compared with control embryos, indicating reduced proliferation or cell death (Fig. 3E, F). At E5.5, 85% of cells were labeled in control embryos compared with 50% of cells in mutant embryos. At E6.5, 100% of cells were labeled in control embryos compared with 85% in mutant embryos. At E7.5 control embryos still showed 100% of cells labeled, but only 30 to 50% of cells were labeled in mutant embryos. A decrease in cell proliferation or induction of cell death may explain low incorporation levels in mutant embryos.

The time and extent of cell death were determined in mutant embryos. To observe nuclear fragmentation, one of the characteristic features of programmed cell death, a TUNEL assay was performed on histological sections from E6.5 and E7.5 embryos (Fig. 3G, H). Apoptotic cells were not frequently observed in E6.5 mutant and control embryos and E7.5 control embryos. However, they were easily observed in the epiblasts of E7.5 mutant embryos. Therefore, reduced levels of BrdU incorporation in E5.5 and E6.5 mutant embryos reflect decreased cell proliferation, while in E7.5 embryos they reflect decreased cell proliferation and increased cell death.

***rad51*^{M1} mutant cells fail to proliferate.** Is embryonic lethality due to a cellular defect? The effect of a homozygous *rad51*^{M1} mutation on cell viability was tested. Two approaches were used to generate *rad51*$^{M1-/-}$ cells. The first was to target both copies of *MmRAD51* in ES cells, and the second was to derive mutant ES cells from cultured blastocysts.

We attempted to mutate both copies of *MmRAD51* in ES cells by sequential rounds of gene targeting. Three different vectors were used: DVpuro, DVpuro2, and DVhygro (Fig. 1A). Two clones of ES cells, targeted first with DVhygro (selected in hygromycin) (Fig. 1C), were transfected with DVpuro (Fig. 1B) or DVpuro2 (Fig. 1D) to target the remaining wild-type copy (selected in puromycin). However, all the clones retargeted the previously mutated copy (63 clones for DVpuro; 8 clones for DVpuro2). This result suggests that homozygous mutant cells failed to proliferate and/or were nonviable.

Cell proliferation and viability were tested with *rad51*$^{M1-/-}$ blastocysts grown in tissue culture. Blastocysts are composed of two cell types, pluripotent cells in the inner cell mass and trophectoderm cells (for reviews, see references 34 and 39). When control blastocysts were grown in tissue culture, cells derived from the inner cell mass became highly proliferative and cells derived from the trophectoderm (trophoblast-like cells) became relatively quiescent. *rad51*$^{M1+/-}$ mice were crossed, and blastocysts were recovered 3.5 days later. Blastocysts were grown in tissue culture to observe the outgrowth of cells derived from the inner cell mass and trophectoderm with a light microscope over 7 days (blastocysts were isolated on day 0). Mutant and control blastocysts attached to the plate at high frequencies. Cells derived from the inner cell mass grew continuously for control but not mutant attached embryos (18 control and 6 mutant embryos observed) (Fig. 4A, B). The number of trophoblast-like cells was the same for both mutant and control attached embryos (30 to 45 cells). The trophoblast-like cells could be maintained because of their relatively quiescent state and/or because of endoreduplication of DNA that may act as a buffer against spontaneous DNA damage.

Analysis of *rad51*$^{M1-/-}$ embryos in utero and in tissue culture demonstrated reduced cell proliferation. Mutant cells were abnormal in embryos at the first time point observed by histology (E5.5), demonstrating that problems occurred earlier. However, it is interesting that most mutant embryos developed to the early egg cylinder stage in spite of the severe cellular phenotype. It is possible that a maternal component briefly rescued mutant preimplantation embryos. *MmRAD51* was shown to be expressed at high levels in the adult ovary (53), and the protein was localized to oocytes during meiosis (3) and to follicle cells in ovaries (88), suggesting the presence of a maternal component.

***rad51*^{M1} mutant cells are hypersensitive to gamma radiation.** Since MmRad51 is homologous to the recombinational repair proteins RecA and ScRad51, it is possible that decreased proliferation was due to a defect in DNA repair. The role of MmRad51 in repairing DNA damage generated by gamma radiation was investigated in trophoblast-like cells derived from E3.5 embryos isolated after heterozygous matings. The isolated blastocysts were exposed to 0, 200, and 400 rads and then allowed to attach to tissue culture plates (day 0). Seven days later the numbers of trophoblast-like cells were counted. There were 30 to 45 trophoblast-like cells without exposure to radiation for both control and mutant attached embryos (nine control and five mutant embryos observed) (Fig. 4A, B). The control trophoblast-like cells were unaffected after exposure to 200 rads (19 control embryos) (Fig. 4C). However, the mutant trophoblast-like cells were reduced in number by 60 to 70% (the range was 10 to 17 cells for seven mutant embryos) (Fig. 4D). There was a slight reduction in trophoblast-like cell number when the control blastocysts were exposed to 400 rads (the range was 20 to 34 cells for 12 control embryos) (Fig. 4E). However, the mutant embryos failed to attach to the plate (three mutant embryos observed) (Fig. 4F). These were the only floating embryos, and the failure to attach was shown to correlate with a dose-dependent response to radiation similar to that exhibited by the outgrowth of trophoblast-like cells (26).

rad51$^{M1+/-}$ trophoblast-like cells did not appear to be more sensitive to gamma radiation than did wild-type cells. In addition, no difference was observed in the survival fractions of *rad51*$^{M1+/-}$ and wild-type ES cells after exposure to gamma radiation (data not shown). Therefore, it is unlikely that the *rad51*^{M1} mutation is dominant or that the heterozygous condition resulted in a significant reduction in protein.

***rad51*$^{M1-/-}$ cells have reduced DNA content.** It is possible that reduced cell proliferation, increased programmed cell death, and hypersensitivity to gamma radiation were due to unrepaired genetic damage, possibly DSB. In yeast cells, unrepaired DSB were shown to reduce DNA content by chromosomal deletion (50, 61). Therefore, metaphase spreads were performed to count chromosomes. Cells were disaggregated

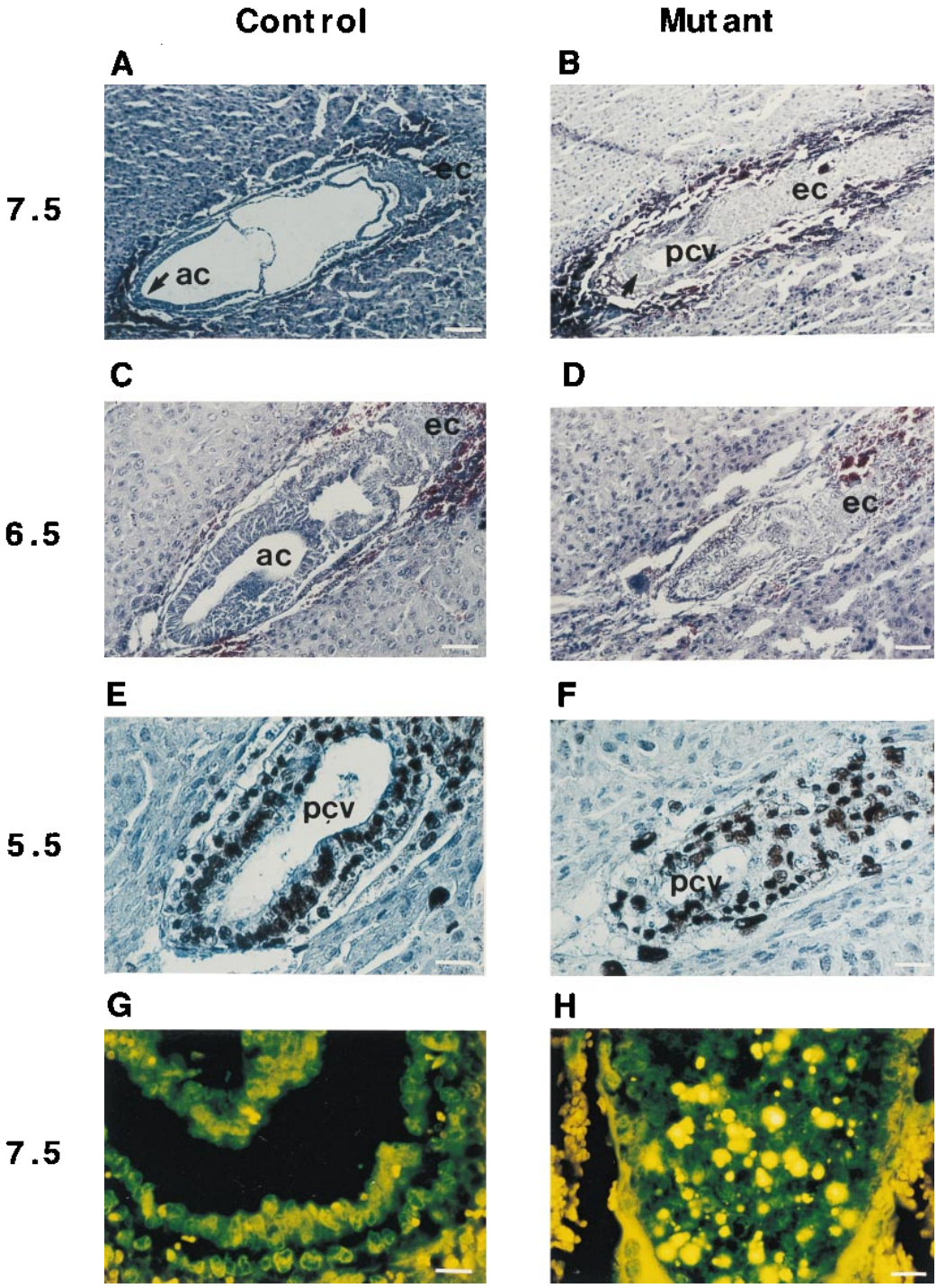

FIG. 3. Histological analysis of control and *rad51*$^{M1-/-}$ embryos. (A, C, E, and G) Control embryos; (B, D, F, and H) mutant embryos. (A and B) Hematoxylin- and eosin-stained E7.5 embryos. ac, amniotic cavity; pcv, proamniotic cavity; ec, ectoplacental cone. The arrow points to an epiblast. (C and D) Hematoxylin- and eosin-stained E6.5 embryos. (E and F) BrdU labeling of E5.5 embryos. (G and H) TUNEL assay of E7.5 embryos displayed in panels A and B. The epiblast region is shown (arrow in panels A and B). Scale bars: panels A and B, 120 μm; panels C and D, 60 μm; panels E and F, 30 μm; panels G and H, 24 μm.

from E7.5 embryos after 2 h of colcemid treatment in utero. Three control embryos were observed individually and five mutant embryos were combined. Mitotic spreads were seen for about half the control cells, and the normal diploid number of chromosomes (40) was observed for 60 out of 60 control cells (Fig. 5A). Unlike control cells, the vast majority of mutant cells were not in mitosis. There were only 10 metaphase spreads out of more than 300 cells. One mutant cell had the normal chromosome number and nine had a little more than half the normal chromosome number (22 to 28) (Fig. 5B). Therefore, most of the mitotically dividing mutant cells displayed multiple chromosome loss.

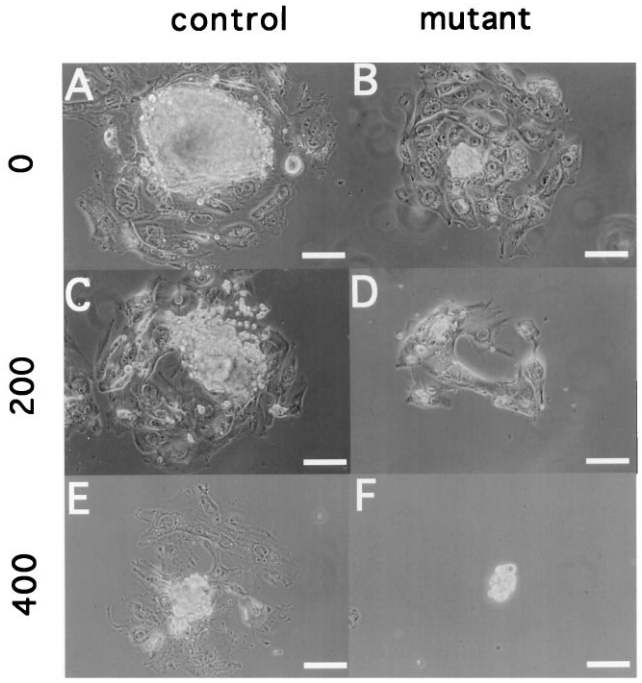

FIG. 4. Exposure of E3.5 embryos to gamma radiation. (A, C, and E) Control embryos; (B, D, and F) mutant embryos. (A and B) No exposure; (C and D) 200-rads exposure; (E and F) 400-rads exposure. Scale bar, 120 μm.

The genetic content was grossly measured in cells throughout the cell cycle in order to observe a larger fraction of the mutant cells. DNA was stained with a fluorescent dye, acridine orange, and the cells were immediately viewed under a fluorescence microscope at 50× magnification under oil immersion. The film was at 400 ASA with the spot setting to focus on a single cell. Genetic content was grossly estimated by fluorescence emission as determined by exposure time; a longer exposure time correlates with less DNA. Cells derived from three control E7.5 embryos were observed individually. Control cells were shown to contain the correct chromosome number during metaphase (as discussed above) and should accurately reflect the normal genetic content found throughout the cell cycle. The range of exposure time was 0.10 to 0.61 s for 48 control cells. Within this range, the exposure times of 71% of the cells were between 0.21 and 0.4 s and those of 46% of cells were between 0.21 and 0.30 s. Cells derived from three mutant E7.5 embryos were observed. The range of exposure time was 0.15 to 2.82 s for 33 mutant cells. The exposure times for 67% of the mutant cells were concentrated between 0.15 and 0.67 s and those for 33% of the mutant cells were between 0.93 and 2.82 s (far out of the range for controls). DNA content may be lost during programmed cell death; however, only two mutant cells appeared apoptotic (condensed chromatin) (28). Low levels of fluorescence, measured by long exposure times, indicated decreased DNA content in a large number of mutant cells throughout the cell cycle.

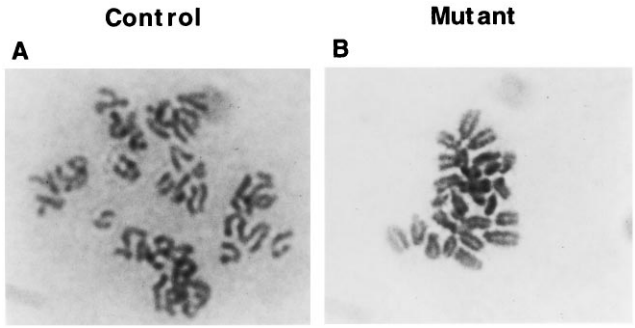

FIG. 5. Metaphase spreads on cells derived from E7.5 embryos. (A) Control; (B) mutant. Magnification, ×650.

TABLE 2. Genotypes[a] and gross morphology for the *rad51*^{m1} and *p53* mutations

E	No. of embryos with indicated *MmRAD51* genotype (gross morphology[b])					
	+/+		+/−		−/−	
	p53$^{+/-}$	*p53*$^{-/-}$	*p53*$^{+/-}$	*p53*$^{-/-}$	*p53*$^{+/-}$	*p53*$^{-/-}$
7.5	0	1 (N)	0	4 (N)	0	1 (N)
8.5	2	4 (N)	9 (N)	12 (N)	5 (R)	6 (S)
9.5	0	1 (N)	0	4 (N)	0	1 (S)

[a] *MmRAD51* and *p53* genotypes were determined by PCR and Southern analysis, respectively, on DNA extracted from the yolk sacs of all embryos except for two of the five resorbed embryos. These two embryos were presumed to be *rad51*$^{M1-/-}$ *p53*$^{+/-}$.

[b] Gross morphology designations: N, normal; S, small; R, resorbed.

Decreased genetic content was clearly observed in a higher percentage of mutant cells during metaphase (90%) than during the complete cell cycle (33%). It is possible that the acridine orange stain failed to detect reduced genetic content in many cells that suffered chromosome loss due to repeated rounds of synthesis without entry into mitosis. In support of this argument, cells were frequently observed in S phase by BrdU labeling but not in mitosis after colcemid treatment of E7.5 mutant embryos.

***rad51*$^{M1-/-}$ embryos survive longer in a p53 mutant background.** It is possible that a cell cycle response to unrepaired DNA damage hindered cell proliferation, induced programmed cell death, and promoted multiple chromosome loss. p53 is commonly believed to be central in delaying DNA replication and stimulating programmed cell death in response to DNA damage, including damage induced by gamma radiation (for a review, see reference 41). The *rad51*^{M1} mutation was crossed into a *p53* mutant background (19). There were no *rad51*$^{M1-/-}$ mice produced out of 41 progeny from a double heterozygote cross or out of 66 progeny from a *p53*$^{-/-}$ *rad51*$^{M1+/-}$ × *p53*$^{+/-}$ *rad51*$^{M1+/-}$ cross. The expected number of *p53*$^{-/-}$ *rad51*$^{M1-/-}$ mice was 11, demonstrating that the *rad51*^{M1} lethal phenotype was not rescued in a *p53* mutant background.

rad51^{M1} mutant embryos were observed in a *p53* mutant background. Development of the *rad51*^{M1} mutant embryos was not observed to change in a *p53*$^{+/-}$ background (Table 2). In a *p53*$^{-/-}$ background, however, *rad51*^{M1} mutant embryos appeared grossly normal at E7.5 and were only slightly smaller than controls at E8.5 (Fig. 6A to E). The head fold had clearly formed in the double-mutant embryos, demonstrating a significant advance in proliferation and development compared with the *rad51*^{M1} mutants in a *p53* wild-type background (Fig. 6D). At E9.5, a double-mutant embryo was not larger in size than at E8.5 and was much smaller than controls.

MEF derived from 11 control and 3 double-mutant E8.5 embryos were observed for proliferation and morphology in tissue culture (controls were *rad51*$^{M1+/+}$ or *rad51*$^{M1+/-}$ in a *p53*$^{-/-}$ background). The MEF were initially plated onto a

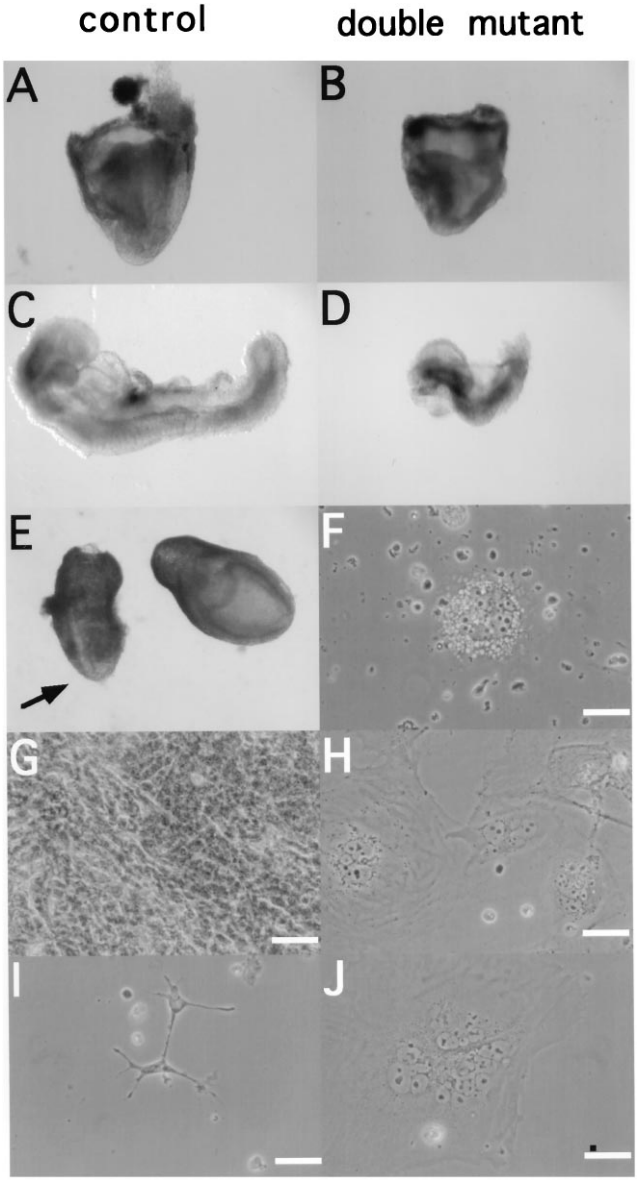

FIG. 6. Morphology of *rad51*$^{M1-/-}$ embryo and MEF in *p53*$^{-/-}$ background. (A) Control (*rad51*$^{M1+/-}$ *p53*$^{+/-}$) and (B) double-mutant E8.5 embryos in yolk sacs. (C) Control and (D) double-mutant E8.5 embryos removed from yolk sacs. (E) Control (*rad51*$^{M1+/-}$ *p53*$^{-/-}$) and double-mutant E7.5 embryos. The arrow points to the double mutant. (F to J) MEF derived from E9.5 embryos. (F) Degenerating double-mutant MEF, passage one; (G) control MEF (*rad51*$^{M1+/-}$ *p53*$^{-/-}$) at high density, passage zero; (H) double-mutant MEF at high density, passage zero; (I) control MEF (*rad51*$^{M1+/-}$ *p53*$^{-/-}$) at low density, passage one; (J) double-mutant MEF at low density, passage one. (A to E) Magnification, ×9.0; (F to J) scale bar, 60 μm.

15-mm-diameter plate (passage zero). Control MEF formed confluent monolayers after 2 to 6 days. The estimated number of cells was about 5×10^5 to 1×10^6 for the control MEF after counting with a hemacytometer. However, the double-mutant MEF were not observed to proliferate and failed to form a confluent monolayer after 6 days in tissue culture. There were not enough cells to count double-mutant MEF with a hemacytometer, so they were counted directly under a light microscope. After 6 days in tissue culture, there were 160, 330, and 1,120 cells for the three double-mutant MEF isolates.

These control and double-mutant MEF were passaged at low density to observe colony formation (passage one). After 14 days in tissue culture the plates were stained with crystal violet to identify colonies of 4 to 16, 17 to 50, and >50 cells. Colonies in these size ranges were frequently observed for all control MEF; however, not one colony was observed for any of the double-mutant MEF, not even a four-cell colony (data not shown).

MEF derived from five control E9.5 embryos and from one double-mutant E9.5 embryo were also observed. All five control MEF formed a confluent monolayer (Fig. 6G). The double-mutant MEF, however, failed to form a confluent monolayer even though they were plated at high density and there was cell-to-cell contact (Fig. 6H). The morphology of control MEF was characteristic of actively proliferating cells (Fig. 6G, I). The morphology of double-mutant MEF (Fig. 6F, H, J), however, was characteristic of differentiating and degenerating cells, indicating premature senescence (7). Senescent cells do not undergo programmed cell death; therefore, an acridine orange stain was performed to observe chromatin condensation, a feature characteristic of apoptotic cells. Chromatin condensation was not observed, further suggesting premature senescence in these double-mutant MEF (data not shown).

DISCUSSION

RecA and ScRad51 were shown to be essential for repair of DSB in bacteria and yeast cells, respectively. Their mouse homolog, *MmRAD51*, was disrupted and found to be important for repair of gamma radiation-induced damage and embryonic development. Mutant embryos arrested at the early egg cylinder stage. There was decreased cellular proliferation followed by programmed cell death, and chromosomes were lost in most mitotically dividing cells by the end of the embryo's life. *rad51*^{M1} mutant embryos survived longer and developed further in a *p53* mutant background; however, fibroblasts derived from double-mutant embryos were unable to proliferate.

Preimplantation lethality was reported for *rad51* mutant embryos by Tsuzuki and colleagues (83). It is unlikely that different genetic backgrounds caused the difference in severity between the phenotypes because both mutations were analyzed in a similar background (albeit the strains may have been slightly different from one colony to another). Different experimental designs may explain the different time points for lethality. Tsuzuki and colleagues extensively analyzed in vitro fertilized and cultured embryos. Possibly, the in vitro environment failed to recapitulate the in vivo environment; perhaps development was slightly delayed, which exacerbated the phenotype. This view is supported by our observation that the inner cellular mass seemed to proliferate less in tissue culture than in utero.

Rad51 performs an essential function in mammalian but not yeast cells. The lethal phenotype reported by both groups was unexpected because mitotically dividing cells deficient for ScRad51 and SpRad51 were viable (56, 75). There are two possible explanations for this discrepancy, which are not mutually exclusive. One is that mammalian Rad51 evolved to perform an essential task. Another is that mammalian Rad51 maintained the same function as yeast Rad51 but that this function is essential in mammalian cells but not in yeast cells.

There is evidence that the RecA homologs perform multiple tasks, some of them not shared by the others. Two RecA homologs were found in *Myxococcus xanthus*; only one was essential, but both complemented UV sensitivity in an *E. coli recA* strain (57). Two RecA homologs found in yeast cells, ScRad51 and DMC1, are essential for meiotic recombination, but only ScRad51 is essential for mitotic recombination (10,

68). In mammals, a DMC1 homolog was isolated, suggesting that RecA homologs possess diverse and unique functions in mammalian cells (30).

MmRad51 may perform a novel role in DNA replication, repair, and/or chromosomal disjunction. *MmRAD51* expression was restricted in the cell cycle to late G_1, S, and G_2, and *MmRAD51* expression was activated by mitogens that induced T- and B-cell proliferation, suggesting a role in replication and repair (88). MmRad51 may take part in disjunction because it was localized to the kinetochores of diakinesis and metaphase 1 chromosomes (3).

Even though it is possible that ablating a unique Rad51 function was responsible for the severe mammalian phenotype, we favor the hypothesis that both mammalian and yeast Rad51 proteins perform a similar function, which is essential for only mammalian cells. *rad51*-mutant mammalian and yeast cells exhibited similar phenotypes. Both cell types were impaired for cell proliferation, were defective in repair of radiation-induced damage, and displayed chromosome loss (49, 56). Each of these aspects of the phenotype can be explained by a defect in DNA repair, specifically recombinational repair. DNA damage was shown to reduce proliferation in both mammalian and yeast cells (for a review, see reference 15), and gamma radiation hypersensitivity suggested that this damage was DSB since DSB are probably the most damaging lesions caused by ionizing radiation (67). Perhaps the most compelling evidence to suggest a failure in the repair of DSB is chromosome deletion. In *S. cerevisiae*, a mutation in either *rad51* or *rad52* stimulated chromosome loss in mitotically dividing diploid cells (49) and exposure to X rays greatly exacerbated this loss to near haploid numbers in *rad52* cells (55). In addition, chromosome loss was observed in diploid yeast cells with a functional recombinational repair pathway; however, these cells were deficient in recombination in one chromosome pair because of divergent homologies over a segment of this chromosome. One of the divergent chromosomes was frequently lost when cells were in G_1 and after exposure to gamma radiation. Thus, homologous recombination and not just ScRad51 function was necessary for chromosomal maintenance (66).

Defective recombinational repair could explain these common pathologies, assuming this function has greater importance in mammalian cells than in yeast cells. The fact that mammalian cells have a much larger genome than yeast cells indicates a more frequent incidence of DSB in mammalian cells and, therefore, a greater need for recombinational repair. If this was the case, then proliferation would be more severely hindered in *rad51*-mutant mammalian cells than in yeast cells because of a greater burden of unrepaired breaks. In support of this argument, mammalian cells were found to be more sensitive to radiation than yeast cells but to display the same sensitivity when their greater genome size was taken into account (22). It is possible that oxidation products spontaneously generate more genetic damage in mammalian cells than in yeast cells, simply because of the larger genome size (for a review, see reference 23).

Therefore, yeast and mammalian cells with a mutation in *rad51* displayed a very similar phenotype, which was characterized by chromosome loss, radiation hypersensitivity, and reduced proliferation. All these aspects to the phenotype could be explained by defective recombinational repair, and the increased severity in mammalian cells could be explained by the greater number of DSB because of the larger genome size.

p53 and a cell cycle response. The early lethal phenotype in *rad51^{M1}*-mutant embryos and cells may be stimulated by a cell cycle response to unrepaired DNA damage. DNA damage was shown to inhibit progression through the cell cycle, thereby demonstrating a relationship between DNA lesions and cell cycle proteins (15). In mitotically dividing budding yeast cells, a single DSB in a dispensable plasmid was sufficient to induce cell death, partly under the control of Rad9 (7, 72, 85). In mammalian cells, the tumor suppressor gene, *p53*, responded to DNA damage induced by gamma radiation by delaying the cell cycle or inducing programmed cell death (38, 43). These responses may be critical in its tumor suppressor function (5, 46, 80). Induction of p53 after exposure to ionizing radiation and to restriction endonucleases suggests that DSB initiated a p53 response (48).

p53 was at least partly responsible for regulating the *rad51^{M1}* phenotype because development was extended from the early egg cylinder stage to the head fold stage in a *p53* mutant background. A multitude of intricate genetic pathways are required at this time in development, and cell proliferation is extremely rapid, demonstrating the need for reasonable genetic integrity. Thus, the damage caused by the *rad51^{M1}* mutation alone must be at levels low enough to permit DNA replication, transcription, and cell division in most cells up to E8.5. The double-mutant embryos died from either an accumulation of DNA damage resulting in metabolic incompetence and mitotic failure or p53-independent regulation.

It is probable that p53 regulates genome surveillance and DNA repair through a myriad of mechanisms, including regulation of transcription and direct interaction with damaged DNA. p53 initiates the transcription of genes that regulate the cell cycle or stimulate programmed cell death, including *p21$^{WAF\text{-}1/CIP\text{-}1/SDI\text{-}1}$* (13, 18, 21, 31, 87) and *BAX* (52), and is critical for the response to gamma radiation-induced DNA damage (20, 47, 48). p53, bound to damaged DNA, may act directly as an early response sensor to arrest the cell cycle or stimulate apoptosis (4, 59).

The C-terminal domain of p53 binds directly to DNA damaged by DNase I, ionizing radiation, and restriction endonucleases (4, 65) and has properties in common with RecA and ScRad51 in vitro. All three recognize and bind to insertion and deletion mismatches (44, 84), catalyze the annealing of complementary single-stranded DNA (17, 59, 86), and catalyze strand transfer (4, 79). Because of these similarities, a synergistic phenotype might be expected in the double-mutant embryos. Since the *rad51^{M1}* phenotype was suppressed by a *p53* mutation, it is doubtful that an intersection of redundant function exists in vivo. However, a loosening of cell cycle control or a delay in programmed cell death brought on by a *p53* mutation may cover up any synergism.

Cellular senescence in double-mutant MEF. The *rad51^{M1}* mutant MEF prematurely became senescent in tissue culture in spite of the *p53* mutation, which in a wild-type background enhanced immortality because of chromosomal instability (32). Cells undergo a limited number of population doublings and arrest at the end of their life spans, termed replicative senescence (14). Since there was a direct correlation between colony forming potential, the age of the cells, and the organism from which they were derived (76, 77), it was not surprising that double-mutant MEF derived from embryos at the end of their life spans failed to proliferate and form colonies. Some theorize that an accumulation of DNA damage is a critical feature of the aging process (71). It is interesting to note that the mutated gene cloned from patients with Werner's syndrome, *WTN*, resembles a DNA helicase, which suggests a defect in DNA metabolism (90). It is possible that a failure in DNA repair accelerated replicative senescence in the highly proliferative cells of *rad51^{M1}* embryos and contributed to embryonic mortality.

Comparison of MmRad51 and DNA-dependent protein kinase-deficient mice. It has been proposed that two recombination pathways are present in mammalian cells, a homologous pathway between sister chromatids that predominantly occurs during S and G_2 and a nonhomologous pathway that predominantly occurs during G_1. The nonhomologous recombination pathway was thought to be the major pathway. Much of this belief stems from gene targeting data that demonstrated homologous recombination to be less frequent than random or illegitimate recombination (12). Other data demonstrated that chromosomal DSB frequently were joined without homology or with only very short stretches of homology (70). DNA-dependent protein kinase (DNA-PK) is critical for nonhomologous but not homologous repair of DSB (45). A biphasic response to ionizing radiation was observed in DNA-PK-deficient cell lines with resistance in late S phase, suggesting that DNA-PK functions in G_1 and that another repair pathway functions in S phase (37). DNA-PK is composed of a catalytic subunit called DNA-PK$_{CS}$ and a DNA end-binding subunit called Ku which is a heterodimer of Ku70 and Ku86 (for a review, see reference 69). Analysis of DNA-PK activity has come from scid (severe combined immunodeficient) mice which are deficient in DNA-PK$_{CS}$ (40) and Ku86-deficient mice (58, 91). Both scid and Ku86-deficient mice are immune deficient because of a defect in the repair of DSB generated during V(D)J recombination. Unfortunately, it is impossible to analyze V(D)J recombination in *rad51*-mutant mice or cells; however, it is unlikely that MmRad51 plays a role in this process since it is localized to the nucleus in late G_1 through G_2 (88) and V(D)J recombination occurs in G_0 or G_1 (73). scid and Ku86-deficient cells do have similarities to MmRad51-deficient cells. All are hypersensitive to ionizing radiation, and Ku86-deficient cells were prematurely senescent in tissue culture, indicating a similar function. However, since scid and Ku86-deficient mice and cells were viable and MmRad51-deficient cells were not, the consequences of removing the putative homologous recombination pathway to repair DSB appear to be much greater than those of removing the nonhomologous pathway.

Future studies. The *rad51*^{M1} mutation proved to be difficult to study because of the severe phenotype. A greater understanding of MmRad51 function may be obtained by selective tissue-specific knockouts or by varying expression levels with an inducible promoter. In addition, crossing the *rad51*^{M1} mutation to alternative genetic backgrounds may prolong life span, as did the *p53*$^{-/-}$ background. Such studies will reveal the molecules that stimulate lethality and delineate the molecules responsible for the different phenotypic features of reduced cell proliferation, programmed cell death, and chromosome deletion.

ACKNOWLEDGMENTS

We thank Robert Wright for his excellent technical assistance; Allan Bradley and his laboratory for the gift of PGKpurobpA, puromycin-resistant SNL6 feeder cells, and AB1 cells; Yuji Mishina and Richard R. Behringer for advice on embryo manipulation and the gift of PGKhygrobpA and hygromycin-resistant feeder cells; Timothy J. McDonnell for advice on cell death morphology; Allan Bradley and Larry Donehower for p53 mutant mice; Roger A. Pedersen for stimulating discussions; and Gigi Lozano, Roger A. Pedersen, and Robert Wright for critical review of the manuscript.

This work was supported by a March of Dimes Basil O'Connor award and a M. D. Anderson Cancer Center PRS research award.

REFERENCES

1. **Aboussekhra, A., R. Chanet, A. Adjiri, and F. Fabre.** 1992. Semidominant suppressors of Srs2 helicase mutations of *Saccharomyces cerevisiae* map in the *RAD51* gene, whose sequence predicts a protein with similarities to procaryotic RecA proteins. Mol. Cell. Biol. **12:**3224–3234.
2. **Adra, C. N., P. H. Boer, and M. W. McBurney.** 1987. Cloning and expression of the mouse pgk-1 gene and the nucleotide sequence of its promoter. Gene **60:**65–74.
3. **Ashley, T., A. W. Plug, J. Xu, A. J. Solari, G. Reddy, E. I. Golub, and D. C. Ward.** 1995. Dynamic changes in Rad51 distribution on chromatin during meiosis in male and female vertebrates. Chromosoma **104:**19–28.
4. **Bakalkin, G., T. Yakovleva, G. Selivanova, K. P. Magnusson, L. Szekely, E. Kiseleva, G. Klein, L. Terenius, and K. G. Wiman.** 1994. p53 binds single-stranded DNA ends and catalyzes DNA renaturation and strand transfer. Proc. Natl. Acad. Sci. USA **91:**413–417.
5. **Baker, S. J., S. Markowitz, E. R. Fearon, J. K. V. Willson, and B. Vogelstein.** 1990. Suppression of human colorectal carcinoma cell growth by wild-type p53. Science **249:**912–915.
6. **Basile, G., M. Aker, and R. K. Mortimer.** 1992. Nucleotide sequence and transcriptional regulation of the yeast recombinational repair gene *RAD51*. Mol. Cell. Biol. **12:**3235–3246.
7. **Bennett, C. B., A. L. Lewis, K. K. Baldwin, and M. A. Resnick.** 1993. Lethality induced by a single site-specific double-strand break in a dispensable yeast plasmid. Proc. Natl. Acad. Sci. USA **90:**5613–5617.
8. **Benson, F. E., A. Stasiak, and S. C. West.** 1994. Purification and characterization of the human RAD51 protein, and analogue of E. coli RecA. EMBO J. **13:**5764–5771.
9. **Bezzubova, O., A. Shinohara, R. G. Mueller, H. Ogawa, and J.-M. Buerstedde.** 1993. A chicken RAD51 homologue is expressed at high levels in lymphoid and reproductive organs. Nucleic Acids Res. **21:**1577–1580.
10. **Bishop, D. K.** 1994. RecA homologs Dmc1 and Rad51 interact to form multiple nuclear complexes prior to meiotic chromosome synapsis. Cell **79:**1081–1092.
11. **Blochlinger, K., and H. Diggelmann.** 1984. Hygromycin B phosphotransferase as a selectable marker for DNA transfer experiments with higher eucaryotic cells. Mol. Cell. Biol. **4:**2929–2931.
12. **Bradley, A., P. Hasty, A. Davis, and R. Ramirez-Solis.** 1992. Modifying the mouse: design and desire. Bio/Technology **10:**534–539.
13. **Brugarolas, J., C. Chandrasekaran, J. I. Gordon, D. Beach, T. Jacks, and G. J. Hannon.** 1995. Radiation-induced cell cycle arrest compromised by p21 deficiency. Nature (London) **377:**552–557.
14. **Campisi, J., G. Dimri, and E. Hara.** 1996. Control of replicative senescence, p. 121–149. *In* E. L. Schneider and J. W. Rowe (ed.), Handbook of the biology of aging. Academic Press, San Diego, Calif.
15. **Carr, A. M., and M. F. Hoekstra.** 1995. The cellular responses to DNA damage. Trends Cell Biol. **5:**32–40.
16. **Cleaver, J. E.** 1994. It was a very good year for DNA repair. Cell **76:**1–4.
17. **Cox, M. M., and I. R. Lehman.** 1981. Directionality and polarity in recA protein-promoted branch migration. Proc. Natl. Acad. Sci. USA **78:**6018–6022.
18. **Deng, C., P. Zhang, J. W. Harper, S. J. Elledge, and P. Leder.** 1995. Mice lacking p21$^{CIP1/WAF1}$ undergo normal development, but are defective in G1 checkpoint control. Cell **82:**675–684.
19. **Donehower, L. A., M. Harvey, B. L. Slagle, M. J. McArthur, C. A. J. Montgomery, J. S. Butel, and A. Bradley.** 1992. Mice deficient for p53 are developmentally normal but susceptible to spontaneous tumours. Nature (London) **356:**215–221.
20. **Dulic, V., W. K. Kaufmann, S. J. Wilson, T. D. Tlsty, E. Lees, J. W. Harper, S. J. Elledge, and S. I. Reed.** 1994. p53-dependent inhibition of cyclin-dependent kinase activities in human fibroblasts during radiation-induced G1 arrest. Cell **76:**1013–1023.
21. **El-Deiry, W. S., T. Tokino, V. E. Velculescu, D. B. Levy, R. Parsons, J. M. Trent, D. Lin, E. Mercer, K. W. Kinzler, and B. Vogelstein.** 1993. WAF1, a potential mediator of p53 tumor suppression. Cell **75:**817–825.
22. **Frankenberg-Schwager, M., and D. Frankenberg.** 1990. DNA double-strand breaks: their repair and relationship to cell killing in yeast. Int. J. Radiat. Biol. **58:**569–575.
23. **Friedberg, E. C., G. C. Walker, and W. Siede.** 1995. DNA repair and mutagenesis. American Society for Microbiology, Washington, D.C.
24. **Game, J. C.** 1983. Radiation-sensitive mutants and repair in yeast, p. 109–137. *In* J. F. T. Spencer et al. (ed.), Yeast genetics: fundamental and applied aspects. Springer-Verlag, Berlin.
25. **Gavrieli, Y., Y. Sherman, and S. A. Ben-Sasson.** 1992. Identification of programmed cell death in situ via specific labeling of nuclear DNA fragmentation. J. Cell Biol. **119:**493–501.
26. **Goldstein, L. S., A. I. Spindle, and R. A. Pedersen.** 1975. X-ray sensitivity of the preimplantation mouse embryo *in vitro*. Radiat. Res. **62:**276–287.
27. **Graham, A., I. Heyman, and A. Lumsden.** 1993. Even-numbered rhombomeres control the apoptotic elimination of neural crest cells from odd-numbered rhombomeres in the chick hindbrain. Development **119:**233–245.
28. **Haaf, T., E. I. Golub, F. Reddy, C. M. Radding, and D. C. Ward.** 1995. Nuclear foci of mammalian Rad51 recombination protein in somatic cells after DNA damage and its localization in synaptonemal complexes. Proc. Natl. Acad. Sci. USA **92:**2298–2302.

29. **Haber, J. E.** 1992. Mating-type gene switching in Saccharomyces cerevisiae. Trends Genet. **8:**446–452.
30. **Habu, T., T. Taki, A. West, Y. Nishimune, and T. Morita.** 1996. The mouse and human homologs of DMC1, the yeast meiosis-specific homologous recombination gene, have a common unique form of exon-skipped transcript in meiosis. Nucleic Acids Res. **24:**470–477.
31. **Harper, J., G. Adami, N. Wei, K. Keyomarsi, and S. Elledge.** 1993. The p21 cdk-interacting protein cip1 is a potent inhibitor of G1 cyclin-dependent kinases. Cell **75:**805–816.
32. **Harvey, M., A. T. Sands, R. S. Weiss, M. E. Hegi, R. W. Wiseman, P. Pantazis, B. C. Giovanella, M. A. Tainsky, A. Bradley, and L. A. Donehower.** 1993. *In vitro* growth characteristics of embryo fibroblasts isolated from p53-deficient mice. Oncogene **8:**2457–2467.
33. **Hayashi, Y., M. Koike, M. Matsutani, and T. Hoshino.** 1988. Effects of fixation time and enzymatic digestion on immunochemical demonstration of bromodeoxyuridine in formalin-fixed, paraffin-embedded tissue. J. Histochem. Cytochem. **36:**511–514.
34. **Hogan, B., R. Beddington, F. Constantini, and E. Lacy.** 1994. Manipulating the mouse embryo, 2nd ed. Cold Spring Harbor Laboratory Press, Cold Spring Harbor, N.Y.
35. **Imamoto, A., and P. Soriano.** 1993. Disruption of the csk gene, encoding a negative regulator of Src family tyrosine kinases, leads to neural tube defects and embryonic lethality in mice. Cell **73:**1117–1124.
36. **Jang, Y. K., Y. H. Jin, F. Fabre, S. H. Hong, and S. D. Park.** 1994. Cloning and sequence analysis of rhp51+, a Schizosaccharomyces pombe homolog of the Saccharomyces cerevisiae RAD51 gene. Gene **142:**207–211.
37. **Jeggo, P. A.** 1990. Studies on mammalian mutants defective in rejoining double-strand breaks in DNA. Mutat. Res. **239:**1–16.
38. **Kastan, M. B., O. Onyekwere, D. Sidransky, B. Vogelstein, and R. W. Craig.** 1991. Participation of p53 protein in the cellular response to DNA damage. Cancer Res. **51:**6304–6311.
39. **Kaufman, M. H.** 1992. The atlas of mouse development, U.S. ed. Academic Press, Inc., San Diego, Calif.
40. **Kirchgessner, C. U., C. K. Patil, J. W. Evans, C. A. Cuomo, L. M. Fried, T. Carter, M. A. Oettinger, and J. M. Brown.** 1995. DNA-dependent kinase (p350) as a candidate gene for the murine SCID defect. Science **267:**1178–1182.
41. **Ko, L., and C. Prives.** 1996. p53: puzzle and paradigm. Genes Dev. **10:**1054–1072.
42. **Krasin, F., and F. Hutchinson.** 1977. Repair of DNA double-strand breaks in Escherichia coli, which requires recA function and the presence of a duplicate genome. J. Mol. Biol. **116:**81–98.
43. **Kuerbitz, S. J., B. S. Plunkett, W. V. Walsh, and M. B. Kastan.** 1992. Wild-type p53 is a cell cycle checkpoint determinant following irradiation. Proc. Natl. Acad. Sci. USA **89:**7491–7495.
44. **Lee, S., B. Elenbaas, A. Levine, and J. Griffith.** 1995. p53 and its 14 kDa C-terminal domain recognize primary DNA damage in the form of insertion/deletion mismatches. Cell **81:**1013–1020.
45. **Liang, F., P. J. Romanienko, D. T. Weaver, P. A. Jeggo, and M. Jasin.** 1996. Chromosomal double-strand break repair in Ku80-deficient cells. Proc. Natl. Acad. Sci. USA **93:**8929–8933.
46. **Lowe, S. W., S. Bodis, A. McClatchey, L. Remington, H. E. Ruley, D. E. Fisher, D. E. Housman, and T. Jacks.** 1994. p53 status and the efficacy of cancer therapy in vivo. Science **266:**807–810.
47. **Lowe, S. W., E. M. Schmitt, S. W. Smith, B. A. Osborne, and T. Jacks.** 1993. p53 is required for radiation-induced apoptosis in mouse thymocytes. Nature (London) **362:**847–849.
48. **Lu, X., and D. P. Lane.** 1993. Differential induction of transcriptionally active p53 following UV or ionizing radiation: defects in chromosome instability syndromes? Cell **75:**765–778.
49. **Malkova, A., E. L. Ivanov, and J. E. Haber.** 1996. Double-strand break repair in the absence of RAD51 in yeast: a possible role for break-induced DNA replication. Proc. Natl. Acad. Sci. USA **93:**7131–7136.
50. **Mansour, S. L., K. R. Thomas, and M. R. Capecchi.** 1988. Disruption of the proto-oncogene *int-2* in mouse embryo-derived stem cells: a general strategy for targeting mutations to non-selectable genes. Nature (London) **336:**348–352.
51. **Mielke, C., M. Tummler, and J. Bode.** 1995. A simple assay for puromycin N-acetyltransferase: selectable marker and reporter. Trends Genet. **11:**258–259.
52. **Miyashita, T., and J. C. Reed.** 1995. Tumor suppressor p53 is a direct transcriptional activator of the human *bax* gene. Cell **80:**293–299.
53. **Morita, T., Y. Yoshimura, A. Yamamoto, K. Murata, M. Mori, H. Yamamoto, and A. Matsuhiro.** 1993. A mouse homolog of the Escherichia coli recA and Saccharomyces cerevisiae RAD51 genes. Proc. Natl. Acad. Sci. USA **90:**6577–6580.
54. **Mortimer, R. K.** 1958. Radiobiological and genetic studies on a polyploid series (haploid to hexaploid) of *Saccharomyces cerevisiae*. Radiat. Res. **9:**312–316.
55. **Mortimer, R. K., R. Contonpoulou, and D. Schild.** 1981. Mitotic chromosome loss in radiation-sensitive strain of the yeast Saccharomyces cerevisiae. Proc. Natl. Acad. Sci. USA **78:**5778–5782.
56. **Muris, D. F. R., K. Vreeken, A. M. Carr, B. C. Broughton, A. R. Lehmann, P. H. M. Lohman, and A. Pastink.** 1993. Cloning the RAD51 homologue of Schizosaccharomyces pombe. Nucleic Acids Res. **21:**4586–4591.
57. **Norioka, N., M.-Y. Hsu, S. Inouye, and M. Inouye.** 1995. Two *recA* genes in *Myxococcus xanthus*. J. Bacteriol. **177:**4179–4182.
58. **Nussenzweig, A., C. Chen, C. D. C. Soares, M. Sanchez, K. Sokol, M. C. Nussenzweig, and G. C. Li.** 1996. Requirement for Ku80 in growth and immunoglobulin V(D)J recombination. Nature (London) **382:**551–555.
59. **Oberosler, P., P. Holoch, U. Ramsperger, and H. Stahl.** 1993. p53-catalyzed annealing of complementary single-stranded nucleic acids. EMBO J. **12:**2389–2396.
60. **Ogawa, T., X. Yu, A. Shinohara, and E. H. Egelman.** 1993. Similarity of the yeast RAD51 filament to the bacterial RecA filament. Science **259:**1896–1899.
61. **Petes, T. D., R. E. Malone, and L. S. Symington.** 1991. Recombination in yeast, p. 407–521. *In* J. R. Broach, J. R. Pringle, and E. W. Jones (ed.), The molecular and cellular biology of the yeast Saccharomyces: genome dynamics, protein synthesis, and energetics. Cold Spring Harbor Laboratory Press, Cold Spring Harbor, N.Y.
62. **Pfarr, D. S., L. A. Rieser, R. P. Woychik, F. M. Rottman, M. Rosenberg, and M. E. Reff.** 1986. Differential effects of polyadenylation regions on gene expression in mammalian cells. DNA **5:**115–122.
63. **Radding, C. M.** 1991. Helical interactions in homologous pairing and strand exchange driven by RecA protein. J. Biol. Chem. **266:**5355–5358.
64. **Ramirez-Solis, R., J. Rivera-Perez, J. D. Wallace, M. Wims, H. Zheng, and A. Bradley.** 1992. Genomic DNA microextraction: a method to screen numerous samples. Anal. Biochem. **201:**331–335.
65. **Reed, M., B. Woelker, P. Wang, Y. Wang, M. E. Anderson, and P. Tegtmeyer.** 1995. The C-terminal domain of p53 recognizes DNA damaged by ionizing radiation. Proc. Natl. Acad. Sci. USA **92:**9455–9459.
66. **Resnick, M. A., M. Skaanild, and T. Nilsson-Tillgren.** 1989. Lack of DNA homology in a pair of divergent chromosomes greatly sensitizes them to loss by DNA damage. Proc. Natl. Acad. Sci. USA **86:**2276–2280.
67. **Ritter, M. A., and J. Cleaver.** 1977. High-LET radiations induce a large proportion of non-rejoining DNA breaks. Nature (London) **266:**653–655.
68. **Rockmill, B., M. Sym, H. Scherthan, and G. S. Roeder.** 1995. Roles for two RecA homologs in promoting meiotic chromosome synapsis. Genes Dev. **9:**2684–2695.
69. **Roth, D. B., T. Lindahl, and M. Gellert.** 1995. How to make ends meet. Curr. Biol. **5:**496–99.
70. **Rouet, P., F. Smih, and M. Jasin.** 1994. Introduction of double-strand breaks into the genome of mouse cells by expression of a rare-cutting endonuclease. Mol. Cell. Biol. **14:**8096–8106.
71. **Roy, A. K., and B. Chatterjee.** 1985. Molecular aspects of aging. Mol. Aspects Med. **8:**1–88.
72. **Schiestl, R. H., P. Reynolds, S. Prakash, and L. Prakash.** 1989. Cloning and sequence analysis of the *Saccharomyces cerevisiae RAD9* gene and further evidence that its product is required for cell cycle arrest induced by DNA damage. Mol. Cell. Biol. **9:**1882–1896.
73. **Schlissel, M., A. Constantinescu, T. Morrow, M. Baxter, and A. Peng.** 1993. Double-strand signal sequence breaks in *V(D)J* recombination are blunt, 5′-phosphorylated, RAG-dependent, and cell cycle regulated. Genes Dev. **7:**2520–2532.
74. **Shinohara, A., H. Ogawa, Y. Matsuda, N. Ushio, K. Ikeo, and T. Ogawa.** 1993. Cloning of human, mouse and fission yeast recombination genes homologous to RAD51 and recA. Nat. Genet. **4:**239–243.
75. **Shinohara, A., H. Ogawa, and T. Ogawa.** 1992. Rad51 protein involved in repair and recombination in S. cerevisiae is a RecA-like protein. Cell **69:**457–470.
76. **Smith, J. R., O. M. Pereira-Smith, K. I. Braunschwieger, T. W. Roberts, and R. G. Whitney.** 1980. A general method for determining the replicative age of normal animal cell cultures. Mech. Ageing Dev. **12:**355–365.
77. **Smith, J. R., O. M. Pereira-Smith, and E. L. Schneider.** 1978. Colony size distributions as a measure of in vivo and in vitro aging. Proc. Natl. Acad. Sci. USA **75:**1353–1356.
78. **Sung, P.** 1994. Catalysis of ATP-dependent homologous DNA pairing and strand exchange by yeast RAD51 protein. Science **265:**1241–1243.
79. **Sung, P., and D. L. Robberson.** 1995. DNA strand exchange mediated by a RAD51-ssDNA nucleoprotein filament with polarity opposite to that of RecA. Cell **82:**453–461.
80. **Symonds, H., L. Krall, L. Remington, M. Saenz-Robles, S. Lowe, T. Jacks, and T. Van Dyke.** 1994. p53-dependent apoptosis suppresses tumor growth and progression in vivo. Cell **78:**703–711.
81. **Tarkowski, A. K.** 1966. An air-drying method for chromosome preparations from mouse eggs. Cytogenetics **5:**394–400.
82. **Terasawa, M., A. Shinohara, Y. Hotta, H. Ogawa, and T. Ogawa.** 1995. Localization of RecA-like recombination proteins on chromosomes of the lily at various meiotic stages. Genes Dev. **9:**925–934.
83. **Tsuzuki, T., Y. Fujii, K. Sakumi, Y. Tominaga, K. Nakao, M. Sekiguchi, A. Matusuhiro, Y. Yoshimura, and T. Morita.** 1996. Targeted disruption of the Rad51 gene leads to lethality in embryonic mice. Proc. Natl. Acad. Sci. USA **93:**6236–6240.

84. **Wang, Y. H., C. D. Bortner, and J. Griffith.** 1993. RecA binding to bulge- and mismatch-containing DNAs. Certain single base mismatches provide strong signals for RecA binding equal to multiple base bulges. J. Biol. Chem. **268:**17571–17577.
85. **Weinert, T. A., and L. H. Hartwell.** 1988. The *RAD9* gene controls the cell cycle response to DNA damage in *Saccharomyces cerevisiae*. Science **241:** 317–322.
86. **Wu, L., J. H. Bayle, B. Elenbaas, N. P. Pavletich, and A. J. Levine.** 1995. Alternatively spliced forms in the carboxy-terminal domain of the p53 protein regulate its ability to promote annealing of complementary single strands of nucleic acids. Mol. Cell. Biol. **15:**497–504.
87. **Xiong, Y., G. Hannon, H. Zhang, D. Casso, R. Kobayashi, and D. Beach.** 1993. p21 is a universal inhibitor of cyclin kinases. Nature (London) **366:** 701–704.
88. **Yamamoto, A., T. Taki, H. Yagi, T. Habu, K. Yoshida, Y. Yoshimura, K. Yamamoto, A. Matsushiro, Y. Nishimune, and T. Morita.** 1996. Cell cycle-dependent expression of the mouse Rad51 gene in proliferating cells. Mol. Gen Genet. **251:**1–12.
89. **Yoshimura, Y., T. Morita, A. Yamamoto, and A. Matshushiro.** 1993. Cloning and sequence of the human RecA-like gene cDNA. Nucleic Acids Res. **21:**1665.
90. **Yu, C.-E., J. Oshima, Y.-H. Fu, E. M. Wijsman, F. Hisama, R. Alisch, S. Matthews, J. Nakura, T. Miki, S. Ousais, G. M. Martin, J. Mulligan, and G. D. Schellenberg.** 1996. Positional cloning of the Werner's Syndrome gene. Science **272:**258–262.
91. **Zhu, B., M. A. Bogue, D.-S. Lim, P. Hasty, and D. B. Roth.** 1996. Ku86-deficient mice exhibit severe combined immunodeficiency and defective processing of V(D)J recombination intermediates. Cell **86:**379–389.